Mon. Not. R. Astron. Soc. **000**, 1–?? (2012) Printed 9 February 2015 (MN LATEX style file v2.2)

A viscous instability in axially symmetric laminar shear flows

N. Shakura ⋆, K. Postnov
Sternberg Astronomical Institute, Moscow M.V. Lomonosov State University, Universitetskij pr., 13, 119992, Moscow, Russia

Received ... Accepted ...

ABSTRACT
A viscous instability in shearing laminar axisymmetric hydrodynamic flows around a gravitating center is described. In the linearized hydrodynamic equations written in the Boussinesq approximation with microscopic molecular transport coefficients, the instability arises when the viscous dissipation is taken into account in the energy equation. Using the local WKB approximation, we derive a third-order algebraic dispersion equation with two modes representing the modified Rayleigh modes R+ and R-, and the third X-mode. We show that in thin accretion flows the viscosity destabilizes one of the Rayleigh modes in a wide range of wavenumbers, while the X-mode always remains stable. In Keplerian flows, the instability increment is found to be a few Keplerian rotational periods at wavelengths with $kr \sim 10 - 50$. This instability may cause turbulence in astrophysical accretion discs even in the absence of magnetic field.

Key words: hydrodynamics, instabilities, accretion discs

1 INTRODUCTION

The origin of turbulence in accretion discs is an outstanding problem in astrophysics. The dimensionless phenomenological parameter α introduced by Shakura & Sunyaev (1973) for assumed turbulent eddy viscosity and chaotic magnetic fields turned out to be very useful in describing physical properties of accretion discs. Analysis of different observations (e.g., the behaviour of non-stationary accretion discs in X-ray novae (Suleimanov, Lipunova & Shakura 2008) and dwarf-nova and AM CVn stars (Kotko & Lasota 2012)) suggest a rather large values $\alpha \sim 0.3$, indicating the presence of well-developed turbulence in the disc. In Keplerian accretion discs, the angular momentum increases with radius, making the flow stable against small hydrodynamic perturbations according to the classical Rayleigh criterion. When the small magnetic field is present in fully ionized gas, a popular mechanism quenching the instability is the Velikhov-Chandrasekhar magneto-rotational instability (MRI) (Velikhov 1959; Chandrasekhar 1960; Balbus & Hawley 1991) (see Balbus & Hawley (1998) for a detailed review). In spite of being a powerful instability, MRI has its own limitations (see e.g. Goodman & Xu (1994), for discussion of parasiting instabilities and Shakura & Postnov (2014), for discussion of applications to thin Keplerian accretion discs).

As for the purely hydrodynamic case, so far there has been no clear criterion of the hydrodynamic turbulence. In a Keplerian flow, there are different mechanisms for small perturbations growth, such as linear growth of transient perturbations (see the recent study Zhuravlev & Razdoburdin (2014) and references therein), but the transition of these perturbations to turbulence, which is a strongly non-linear process, remains unclear.

In this paper we perform the linear stability analysis of shearing laminar hydrodynamic viscous flows with arbitrary rotation laws in the form $\Omega^2 \propto r^{-n}$ taking into account the viscous heating and thermal conductivity in the energy equation. Unlike many previous works, we use microscopic molecular transport coefficients to describe the viscosity and heat conductivity. These terms in the energy equation make one of the Rayleigh modes unstable (i.e. make their amplitude exponentially growing) in a wide range of wave numbers for perturbations normal to the direction of the wave vector. Physically, the instability may be due to the viscously heated gas being unstable to convection in the gravity field of the central object in the absence of the background entropy gradients.

The instability increment decreases (but does not vanish) with increasing thermal conductivity and is maximum in cold neutral flows with largest Prandtl numbers. We discuss the relevance of the found viscous instability to the generation of turbulence in laminar thin accretion flows.

The pulsational instability of viscous accretion discs was first studied by Kato (1978). The viscous instability of the standard turbulent Shakura-Sunyaev α-discs was investigated in many papers (see, e.g., Blumenthal, Lin & Yang (1984); Kley, Papaloizou & Lin (1993); Latter & Ogilvie (2006), among others). (Note that in the latter papers the viscous instability is referred to as 'viscous overstability', i.e. when arising as an exponentially growing oscillations, in analogy with stellar pulsations discussed by Eddington (1926), and the term 'instability' is reserved for purely imaginary negative modes.)

In Section 2 we derive the basic dispersion equation. To make the physical case as simple as possible, we work in the Boussinesq approximation (i.e. consider the fluid incompressible $\nabla \boldsymbol{u} = 0$, keep the Eulerian pressure variations non-zero only in the equations of motion and put them zero in the energy equation) and take small

⋆ E-mail: nikolai.shakura@gmail.com, kpostnov@gmail.com

perturbations in the form of plane waves in the direction transversal to the wave propagation. For such perturbations we derive a third-order algebaraic dispersion equation with imaginary coefficients, which has three solutions: one Rayleigh mode with positive real part (R+), the Rayleigh mode with negative real part (R-) and a new mode which has zero real and imaginary part at $k \to 0$ (the X-mode). We find that one of the Rayleigh modes becomes unstable (exponentially growing) at large wavelengths, while the X-mode remains stable at all wavelengths. In Section 3 we analyze the obtained the dispersion equation. First we rewrite it in the dimensionless form, and then perform its numerical analysis for several important cases of thermal conductivity (for purely electron conductivity in the fully ionized plasma, for the case where the radiation conductivity is important, and for the case of neutral monoatomic hydrogen gas where the heat conductivity and viscosity are caused by the same particles). In Section 5 we discuss the applicability of the approximation of incompressibility we use and damping of the instability due to entropy gradients in the unperturbed flow. Section 6 summarizes our findings. Details of linearization of the viscous force in the dynamical equations are given in the Appendix.

2 DERIVATION OF THE DISPERSION EQUATION

We start with the linear analysis of hydrodynamic equations. The fluid viscosity and thermal conductivity is taken into account through kinematic viscosity coefficient ν and heat conductivity coefficient κ, respectively.

2.1 Basic equations

The system of hydrodynamic equations reads:

(i) mass conservation equation

$$\frac{\partial \rho}{\partial t} + \nabla \cdot (\rho \boldsymbol{u}) = 0\,, \tag{1}$$

In cylindrical coordinates for axially symmetric flows:

$$\nabla \cdot (\rho \boldsymbol{u}) = \frac{1}{r}\frac{\partial (\rho r u_r)}{\partial r} + \frac{\partial (\rho u_z)}{\partial z} \tag{2}$$

(ii) Navier-Stokes equation including gravity force

$$\frac{\partial \boldsymbol{u}}{\partial t} + (\boldsymbol{u}\nabla)\cdot\boldsymbol{u} = -\frac{1}{\rho}\nabla p - \nabla\phi_g + \boldsymbol{\mathcal{N}}\,. \tag{3}$$

Here $\phi_g = -GM/r$ is the Newtonian gravitational potential of the central body with mass M, $\boldsymbol{\mathcal{N}}$ is the viscous force. In cylindrical coordinates for axisymmetric flows:

$$\frac{\partial u_r}{\partial t} + u_r\frac{\partial u_r}{\partial r} + u_z\frac{\partial u_r}{\partial z} - \frac{u_\phi^2}{r} = -\frac{\partial \phi_g}{\partial r} - \frac{1}{\rho}\frac{\partial p}{\partial r} + \mathcal{N}_r\,, \tag{4}$$

$$\frac{\partial u_\phi}{\partial t} + u_r\frac{\partial u_\phi}{\partial r} + u_z\frac{\partial u_\phi}{\partial z} + \frac{u_r u_\phi}{r} = \mathcal{N}_\phi\,, \tag{5}$$

$$\frac{\partial u_z}{\partial t} + u_r\frac{\partial u_z}{\partial r} + u_z\frac{\partial u_z}{\partial z} = -\frac{\partial \phi_g}{\partial z} - \frac{1}{\rho}\frac{\partial p}{\partial z} + \mathcal{N}_z\,. \tag{6}$$

The linearized viscous force components are specified in Appendix A.

(iii) energy equation

$$\frac{\rho \mathcal{R} T}{\mu}\left[\frac{\partial s}{\partial t} + (\boldsymbol{u}\nabla)\cdot s\right] = Q_{\rm visc} - \nabla\cdot\boldsymbol{F}\,. \tag{7}$$

where s is the specific entropy per particle, $Q_{\rm visc}$ is the viscous dissipation rate per unit volume, $\mathcal{R}$ is the universal gas constant, μ is the molecular weight, T is the temperature, and terms on the right stand for the viscous energy production and the heat conductivity energy flux $\boldsymbol{F}$, respectively. The energy flux due to the heat conductivity is

$$\nabla\cdot\boldsymbol{F} = \nabla(-\kappa\nabla T) = -\kappa\Delta T - \nabla\kappa\cdot\nabla T\,. \tag{8}$$

Note that both electrons and photons, and at low temperatures neutral atoms, can contribute to the heat conductivity (see Section 3 below).

(iv) equation of state

The equation of state for a perfect gas is convenient to write in the form:

$$p = K e^{s/c_V}\rho^\gamma\,, \tag{9}$$

where K is a constant, $c_V = 1/(\gamma-1)$ is the specific volume heat capacity and $\gamma = c_p/c_V$ is the adiabatic index (5/3 for the monoatomic gas).

2.2 Linearization of basic equations

We will consider small axially symmetric perturbations in the WKB approximation with space-time dependence $e^{i(\omega t - k_r r - k_z z)}$, where r, z, ϕ are cylindrical coordinates. The velocity perturbations are $\boldsymbol{u} = (u_r, u_\phi, u_z)$. The density, pressure, temperature and entropy perturbations are ρ_1, p_1, T_1, and s_1 over the unperturbed values ρ_0, p_0, T_0, and s_0, respectively. As a simplification, to filter out acoustic oscillations arising from the restoring pressure force, we will use the Boussinesq approximation, i.e. consider incompressible gas motion $\nabla\cdot\boldsymbol{u} = 0$. In the energy equation we will neglect Eulerian pressure variations, $p_1(t, r, \phi, z) = 0$ (see the justification below), but Lagrangian pressure variations $\delta p(t, r(t_0), \phi(t_0, z(t_0))$ are non-zero. (We remind that for infinitesimally small shifts a perturbed gas parcel acquires the pressure equal to that of the ambient medium; see e.g. Spiegel & Veronis (1960); Kundu, Cohen & Dowling (2012) for discussion of the Boussinesq approximation). We stress that we investigate the motion of axisymmetric transverse perturbations, i.e. small perturbations in the direction normal to the wave vector $\boldsymbol{k}$.

2.2.1 Dynamical equations

In the linear approximation, the system of differential hydrodynamic equations is reduced to the following system of algebraic equations.

a). The Boussinesq approximation for gas velocity $\boldsymbol{u}$ is $\nabla\cdot\boldsymbol{u} = 0$:

$$k_r u_r + k_z u_z = 0\,. \tag{10}$$

b). The radial, azimuthal and vertical components of the Navier-Stokes momentum equation are, respectively:

$$i\omega u_r - 2\Omega u_\phi = ik_r\frac{p_1}{\rho_0} - \frac{\rho_1}{\rho_0^2}\frac{\partial p_0}{\partial r} - \nu k^2 u_r[R]\,, \tag{11}$$

where the factor $[R]$ takes into account the dependence of the viscosity coefficient on temperature $\eta \sim T^{\alpha_{visc}}$ ($\alpha_{visc} = 5/2$ for fully ionized gas and $\alpha_{visc} = 1/2$ for neutral gas) in the perturbed viscous force component $\mathcal{N}_r$ (see Eq. (A16) in Appendix A);

$$i\omega u_\phi + \frac{\varkappa^2}{2\Omega}u_r = -\nu k^2 u_\phi[\Phi]\,, \tag{12}$$

where the factor $[\Phi]$ takes into account variations of the viscosity coefficient in the perturbed viscous force component $\mathcal{N}_\phi$ (see Eq. (A21) in Appendix A);

$$i\omega u_z = ik_z\frac{p_1}{\rho_0} - \frac{\rho_1}{\rho_0^2}\frac{\partial p_0}{\partial z} - \nu k^2 u_z[Z] \tag{13}$$

where the factor $[Z]$ takes into account variations of the viscosity coefficient in the perturbed viscous force component $\mathcal{N}_z$ (see Eq. (**??**) in Appendix A). Here $k^2 = k_r^2 + k_z^2$ and

$$\varkappa^2 = 4\Omega^2 + r\frac{d\Omega^2}{dr} \equiv \frac{1}{r^3}\frac{d\Omega^2 r^4}{dr} \tag{14}$$

is the epicyclic frequency. For the power-law rotation $\Omega^2 \sim r^{-n}$ the epicyclic frequency is simply $\varkappa^2/\Omega^2 = 4 - n$. In deriving these equations we neglected terms $\sim (k_r/r), (k_z/r)$ compared to terms $\sim k^2$, see also the discussion in Acheson (1978).

2.2.2 *Energy equation*

To specify density perturbations ρ_1/ρ_0, the energy equation should be used. In the general case by varying the equation of state Eq. (9) we obtain for entropy perturbations:

$$\frac{p_1}{p_0} = \frac{s_1}{c_V} + \gamma\frac{\rho_1}{\rho_0}\,. \tag{15}$$

On the other hand, from the equation of state for ideal gas in the form $p = \rho\mathcal{R}T/\mu$, we find for small temperature perturbations we have:

$$\frac{p_1}{p_0} = \frac{\rho_1}{\rho_0} + \frac{T_1}{T_0}\,. \tag{16}$$

Substitution of Eq. (15) and Eq. (16) into equations of motion Eq. (11) and Eq. (13) immediately shows that the terms with $(p_1/p_0)k_r$ and $(p_1/p_0)k_z$ in the dynamical equations are larger by factors rk_r and rk_z than terms with p_1/p_0 arisen from the energy equation. This means that in the energy equation we can set Eulerian pressure perturbations equal to zero, as is usually assumed in the Boussinesq approximation, i.e.

$$\frac{s_1}{c_V} + \gamma\frac{\rho_1}{\rho_0} = 0\,. \tag{17}$$

$$\frac{\rho_1}{\rho_0} = -\frac{T_1}{T_0}\,. \tag{18}$$

We repeat again that the Eulerian pressure variations should be retained in the equations of motion (11)- (13). Eq. (18) implies that in the axially symmetric waves considered here the density variations are in counter-phase with temperature variations.

The viscous dissipative function $Q_{\rm visc}$ [erg cm^{-3} s^{-1}] can be written as $Q_{\rm visc} = \rho\nu\Phi$, where the function Φ in polar coordinates is

$$\begin{aligned}\Phi = \quad & 2\left[\left(\tfrac{\partial u_r}{\partial r}\right)^2 + \left(\tfrac{1}{r}\left(\tfrac{\partial u_\phi}{\partial\phi}\right) + \tfrac{u_r}{r}\right)^2 + \left(\tfrac{\partial u_z}{\partial z}\right)^2\right] \\ & + \left[r\tfrac{\partial}{\partial r}\left(\tfrac{u_\phi}{r}\right) + \tfrac{1}{r}\tfrac{\partial u_r}{\partial\phi}\right]^2 + \left[\tfrac{1}{r}\tfrac{\partial u_z}{\partial\phi}\right]^2 \\ & + \left[\tfrac{\partial u_r}{\partial z} + \tfrac{\partial u_z}{\partial r}\right]^2 - \tfrac{2}{3}(\nabla\cdot\boldsymbol{u})^2\,.\end{aligned} \tag{19}$$

All terms but one in this function are quadratic in small velocity perturbations; this term has the form:

$$\nu\rho\left(\frac{\partial u_\phi}{\partial r} - \frac{u_\phi}{r}\right)^2\,. \tag{20}$$

Writing for the azimuthal velocity $u_\phi = u_{\phi,0} + u_{\phi,1}$ (here for the purposes of this paragraph and only here we specially mark the unperturbed velocity with index 0, not to be confused with our notations u_ϕ for perturbed velocity in Eq. (11)-Eq. (12) above and below), we obtain for the viscous dissipation function

$$Q_{\rm visc} = \nu\rho r\frac{d\Omega}{dr}\left[r\frac{d\Omega}{dr} - 2ik_r u_{\phi,1} - 2\frac{u_{\phi,1}}{r}\right] + \text{quadratic terms}\,. \tag{21}$$

Here $\Omega = u_{\phi,0}/r$ is the angular (Keplerian) velocity of the unperturbed flow. The first term in parentheses describes the viscous energy release in the unperturbed Keplerian flow. For this unperturbed flow we have

$$\frac{\partial s_0}{\partial t} = \nu\mu\frac{[r(d\Omega/dr)]^2}{\mathcal{R}T_0} = \frac{9}{4}\nu\mu\frac{\Omega^2}{\mathcal{R}T_0}\,. \tag{22}$$

Thus, the entropy of the unperturbed flow changes along the radius. However, on the scale of the order of or smaller than the disc thickness z_0, the entropy gradient can be neglected. The second term in Eq. (21) vanishes if $k_r = 0$ (and then there are no viscous dissipation effects to linear order), therefore we will consider only two-dimensional transverse perturbations with $k_z \neq 0$, $k_r \neq 0$.

We emphasize that in our analysis we neglect the background entropy gradients, which can be present in real flows, i.e. we will consider the flow in the local neutral equilibrium. This is done to exclude the effects of these gradients on the evolution of small perturbations. As is well known, with inclusion of the background entropy gradients, the Brunt-Väisälä frequencies arise. If their squares are positive, they stabilize perturbations. If their squares are negative, they signal emergence of convection (see, for example, Kato, Fukue & Mineshige (1998), for more detail).

The right side of the heat conductivity equation Eq. (8) for small temperature perturbations, with account for the dependence of the thermal conductivity coefficient on temperature and density $\kappa \sim T^c\rho^d$, in the linear order can be recast to the form

$$\begin{aligned}\kappa\Delta T + \nabla\kappa\cdot\nabla T = -\kappa k^2 T_0\tfrac{T_1}{T_0} - \\ (c-d)\kappa T_0\tfrac{T_1}{T_0}ik_r\tfrac{1}{T_0}\tfrac{\partial T_0}{\partial r} - (c-d)\kappa T_0\tfrac{T_1}{T_0}ik_z\tfrac{1}{T_0}\tfrac{\partial T_0}{\partial z}\,,\end{aligned} \tag{23}$$

(here we have used the relation (18)). It is useful to rewrite the right side of this equation in the form

$$-\kappa k^2 T_0\frac{T_1}{T_0}\left(1 + (c-d)i\frac{k_r}{k^2}\frac{1}{T_0}\frac{\partial T_0}{\partial r} + (c-d)i\frac{k_z}{k^2}\frac{1}{T_0}\frac{\partial T_0}{\partial z}\right) \tag{24}$$

to see that in so far as $\frac{1}{T_0}\frac{\partial T_0}{\partial r} \sim -1/r$, $\frac{1}{T_0}\frac{\partial T_0}{\partial z} \sim -1/z_0$ and that terms $\sim k_r/r$ should be neglected compared to terms $\sim k^2$, only the first term $\sim k^2$ and third term $\sim k_z/z_0$ should be retained in this equation.

Therefore, the energy equation Eq. (7) turns into

$$i\omega\frac{\rho_0\mathcal{R}T_0}{\mu}s_1 = -2ik_r\nu\rho_0 r\frac{d\Omega}{dr}u_\phi - \kappa k^2 T_0\frac{T_1}{T_0}[E]\,, \tag{25}$$

where we have introduced the correction factor

$$[E] = 1 + i(c-d)\left(\frac{k_z}{k^2}\right)\frac{1}{T_0}\frac{\partial T_0}{\partial z}\,.$$

Like in the linearized continuity equation $\nabla\cdot\boldsymbol{u} = 0$, here we have neglected the term u_ϕ/r. The first term in the right side of Eq. (25) corresponds to the energy generation in axially symmetric sheared flow due to viscosity, and the second term means the entropy perturbation smoothing due to heat conductivity. The first term $\sim (k_r/r)(u_{\phi,0}/u_s)^2\eta$, and the second term $\sim k^2\eta/\mathrm{Pr}$, where the Prandtl number is the ratio of the heat conductivity to dynamical viscosity coefficient. While the k_r/r is small relative to k^2, the coefficient $(u_{\phi,0}/u_s)^2$ is very large for thin discs, and therefore the heat generation term should be retained in the energy equation.

2.3 Dispersion equation

By substituting Eq. (17) and Eq. (18) into Eq. (25), we find the relation between the density variations and u_ϕ in the Boussinesq limit with zero background entropy gradients:

$$\frac{\rho_1}{\rho_0}\left(i\omega+\frac{\kappa k^2[E]}{c_p\rho_0\mathcal{R}/\mu}\right)=\frac{2ik_r\nu r(d\Omega/dr)}{c_p\mathcal{R}T_0/\mu}u_\phi\,. \tag{26}$$

Here $c_p=\gamma c_V=\gamma/(\gamma-1)$ is the specific heat capacity (per particle) at constant pressure.

It is convenient to introduce the dimensionless Prandtl number:

$$\mathrm{Pr}\equiv\frac{\nu\rho_0 C_p}{\kappa}=\frac{\nu\rho_0(\mathcal{R}/\mu)c_p}{\kappa}=\frac{\nu\rho_0(\mathcal{R}/\mu)}{\kappa}\frac{\gamma}{\gamma-1}\,. \tag{27}$$

The Prandtl number defined by Eq. (27) for fully ionized hydrogen gas ($\gamma=5/3$), where the heat conduction is determined by light electrons, is quite low (see Spitzer (1962)):

$$\mathrm{Pr_e}\approx\frac{0.406}{20\cdot0.4\cdot0.225\cdot(2/\pi)^{3/2}}\left(\frac{m_e}{m_p}\right)^{1/2}\left(\frac{5}{2}\right)\approx0.052\,. \tag{28}$$

Note also that in this case $d=0$ and $c=5/2$ in the heat conductivity coefficient.

By expressing the heat conductivity coefficient κ through kinematic viscosity coefficient ν using Eq. (27) and after substituting Eq. (26) into Eq. (11), we arrive at:

$$\begin{aligned}ik_r\frac{p_1}{\rho_0}&=(i\omega+\nu k^2[R])u_r+\frac{\varkappa^2}{(i\omega+\nu k^2[\Phi])}u_r\\&-\frac{1}{c_p}\frac{1}{p_0}\frac{\partial p_0}{\partial r}\frac{\varkappa^2 i\nu k_r(d\ln\Omega/d\ln r)}{(i\omega+\nu k^2[\Phi])(i\omega+\nu k^2[E]/\mathrm{Pr})}u_r\,.\end{aligned} \tag{29}$$

Now by substituting Eq. (26) into Eq. (13) with account for Eq. (10), we arrive at

$$\begin{aligned}ik_z\frac{p_1}{\rho_0}&=-\frac{k_r}{k_z}(i\omega+\nu k^2[Z])u_r\\&-\frac{1}{c_p}\frac{1}{p_0}\frac{\partial p_0}{\partial z}\frac{\varkappa^2 i\nu k_r(d\ln\Omega/d\ln r)}{(i\omega+\nu k^2[\Phi])(i\omega+\nu k^2[E]/\mathrm{Pr})}u_r\,.\end{aligned} \tag{30}$$

Finally, by subtracting Eq. (30) multiplied by k_r from Eq. (29) multiplied by k_z we arrive at the dispersion equation:

$$\begin{aligned}&(i\omega+\nu k^2[\Phi])\left[(i\omega+\nu k^2[R])\frac{k_z^2}{k^2}+(i\omega+\nu k^2[Z])\frac{k_r^2}{k^2}\right]\\&+\left(\frac{k_z}{k}\right)^2\varkappa^2\left[1-\frac{\gamma-1}{\gamma}\frac{ik_r}{(i\omega+\nu k^2[E]/\mathrm{Pr})}\left(A-\frac{k_r}{k_z}B\right)\right]=0\,,\end{aligned} \tag{31}$$

where

$$A\equiv\nu\frac{d\ln\Omega}{d\ln r}\frac{1}{p_0}\frac{\partial p_0}{\partial r} \tag{32}$$

$$B\equiv\nu\frac{d\ln\Omega}{d\ln r}\frac{1}{p_0}\frac{\partial p_0}{\partial z} \tag{33}$$

The expression in the square brackets in Eq. (31) above can be rewritten in the equivalent form:

$$\left[1+\frac{\gamma-1}{\gamma}\frac{i\nu}{(i\omega+\nu k^2[E]/\mathrm{Pr})}\frac{d\ln\Omega/d\ln r}{\mathcal{R}T_0/\mu}\left(k_r g_{r,eff}-\frac{k_r^2}{k_z}g_z\right)\right], \tag{34}$$

where $g_{r,eff}=-1/\rho_0(\partial p_0/\partial r)$ and $g_z=-1/\rho_0(\partial p_0/\partial z)$ are the effective radial and vertical gravity accelerations in the unperturbed flow, respectively. Clearly, the term $k_r g_{r,eff}\sim k_r/r$ is much smaller than $(k_r^2/k_z)g_z\sim(k_r^2/k_z)1/z_0$ and will be neglected in the further analysis. Note that if the dynamic viscosity coefficient is independent of temperature (i.e. $\alpha_{visc}=0$), correction factors $[R]=[\Phi]=[Z]=1$ and the first line in Eq. (31) is simplified to $(i\omega+\nu k^2)^2$. We will see below that deviations of these correction factors from unity insignificantly affect the result of our analysis.

3 ANALYSIS OF THE DISPERSION EQUATION

First consider the limiting case where $A=B=0$ and $[R]=[\Phi]=[Z]=1$, i.e. the case where the viscous energy generation in the energy equation is ignored, but the viscosity is retained in the equations of motion. Then Eq. (31) represents the well-known Rayleigh dispersion equation for viscous fluid:

$$(i\omega+\nu k^2)^2=-\left(\frac{k_z}{k}\right)^2\varkappa^2\,, \tag{35}$$

which describes two Rayleigh modes. Depending on the sign of $\varkappa^2$ these modes are oscillating (if the epicyclic frequency $\varkappa^2>0$, the angular momentum increases with radius), or exponentially growing (the unstable Rayleigh mode) and exponentially decaying (if the epicyclic $\varkappa^2<0$, the angular momentum decreases with radius). The arising of the unstable Rayleigh mode corresponds to the classical Rayleigh criterion of instability of a shearing flow. As can be easily seen from Eq. (35), the viscosity stabilizes the unstable mode at short wavelengths (large k). Two solutions of Eq. (35) for typical viscosity parameters discussed below and $\varkappa^2=\Omega^2$ (the Keplerian motion) are shown in the fourth column of Fig. 1.

However, in the general viscous case where $A,B\neq0$, the dispersion equation Eq. (31) turns into a cubic equation, that is, the third mode arises (the X-mode) due to the viscous heating of the fluid. At non-zero A and B, one of the Rayleigh modes (which is stable in the dissipationless case) becomes exponentially unstable in a wide range of wavenumbers. We stress that these modes remain stable for either $k_r=0$ or $k_z=0$. Indeed, the dispersion equation for perturbations with $k_r=0$ is reduced to Eq. (35) above. For perturbations with $k_z=0$, the dispersion equation turns into $i\omega+\nu k_r^2=0$, i.e. is reduced to an exponentially decaying standing wave. We stress that in our case the larger viscosity, the higher instability increment. This is opposite to the situation where a poloidal magnetic field is present, when the magneto-rotational instability is developed: increasing viscosity decreases the MRI increment. Clearly, there is no viscous instability of the Rayleigh modes in the inviscid case ($\nu=0$) or in the shearless case (solid-body rotation with $n=0$).

3.1 Dimensionless dispersion equation

For numerical analysis, the cubic dispersion equation Eq. (31) can be conveniently rewritten in the dimensionless form. To do this, we multiply Eq. (31) through the factor $(i\omega+\nu k^2[E]/\mathrm{Pr})$, divide the obtained equation through Ω^3 and introduce new dimensionless variables:

$$\tilde\omega\equiv\frac{\omega}{\Omega}\,,\quad kr\,,\quad\tilde\varkappa^2\equiv\frac{\varkappa^2}{\Omega^2}. \tag{36}$$

The kinematic viscosity is $\nu=lu_s$, where l is the effective mean free path of ions, $u_s=\sqrt{\gamma\mathcal{R}T_0/\mu}$ is the characteristic velocity in the unperturbed flow which is about thermal velocity of ions, so the dimensionless combination $\nu k^2/\Omega$ becomes:

$$\frac{\nu k^2}{\Omega}=a(kr)^2\,. \tag{37}$$

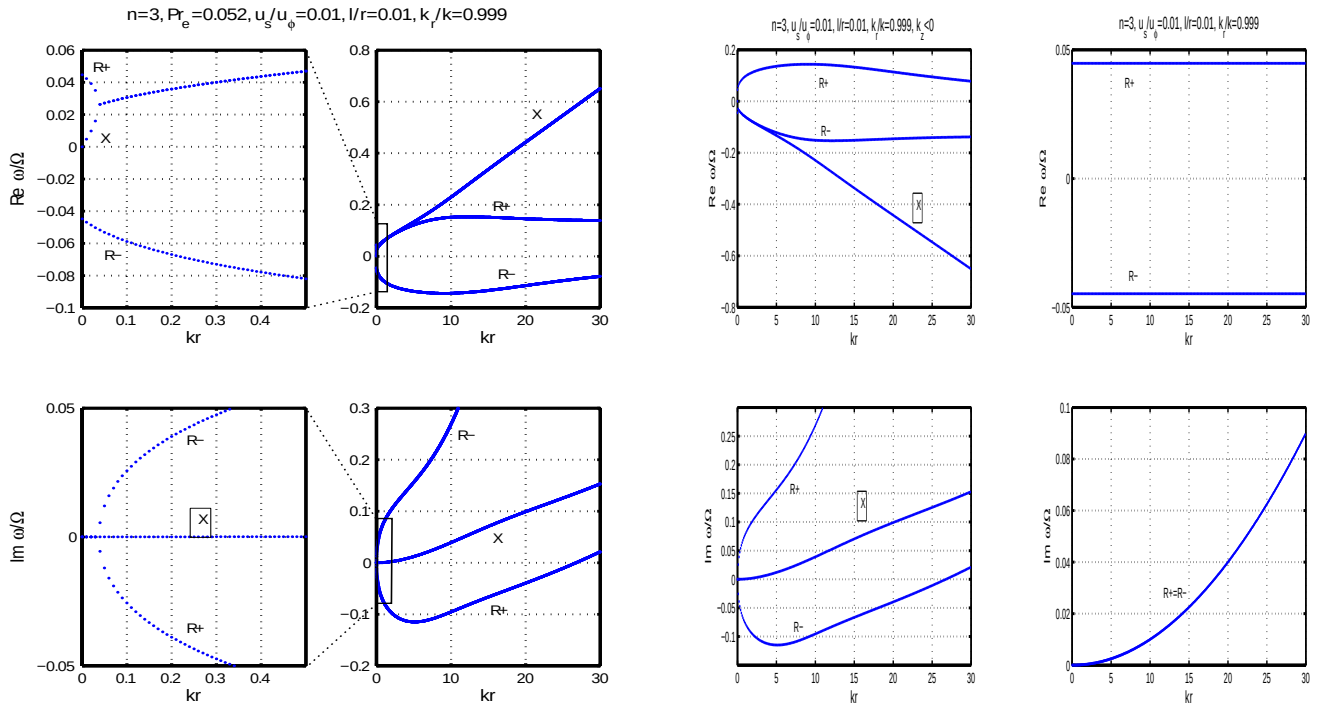

Figure 1. Three modes of dispersion equation (41) for electron thermal conductivity in fully ionized plasma (the Prandtl number Pr_e=0.052). R+ and R- mark two Rayleigh modes, one of which (R+ if $k_z > 0$ and R- if $k_z < 0$) becomes viscously unstable. Upper row: Re$\tilde{\omega}$, bottom row: Im$\tilde{\omega}$. The first two column show the case $k_r/k = 0.999, k_z > 0$. The left column zooms the region of small kr to see the behaviour of three modes as $kr \to 0$: Re and Im parts of the X-mode always starts from zero, while at $kr = 0$ Re and Im parts of the Rayleigh modes is non-zero and zero, respectively. The third column shows the case $k_r/k = 0.999, k_z < 0$: the imaginary part of the modes is unchanged and the real part changes sign. For comparison, the fourth column shows two (stable) Rayleigh modes as the solution of Eq. (35).

Here we have introduced the dimensionless coefficient

$$a \equiv \left(\frac{u_s}{u_\phi}\right)\left(\frac{l}{r}\right). \tag{38}$$

Formally, $1/a$ is the Reynolds number defined as Re$= (u_\phi r)/\nu$, but as we will see below, for a specified Reynolds number, different solutions are realized.

The vertical pressure gradient in coefficient B in Eq. (31) turns into

$$\frac{1}{p_0}\frac{\partial p_0}{\partial z} \to -\frac{1}{z_0}, \tag{39}$$

where z_0 is the characteristic disc height. Using the relation for thin accretion discs

$$\frac{z_0}{r} = \sqrt{\Pi_1/\gamma}\left(\frac{u_s}{u_\phi}\right) \tag{40}$$

(where the dimensionless coefficient Π_1 takes into account the model vertical disc structure, see Ketsaris & Shakura (1998); in numerical calculation below we shall assume $\sqrt{\Pi_1/\gamma} = 2$), we obtain the dispersion equation in the dimensionless form:

$$(i\tilde{\omega} + a(kr)^2[\Phi])\left[(i\tilde{\omega} + a(kr)^2[R])\frac{k_z^2}{k^2} + (i\tilde{\omega} + a(kr)^2[Z])\frac{k_r^2}{k^2}\right]$$
$$+\left(\frac{k_z}{k}\right)^2\tilde{\varkappa}^2\left[1 - i\frac{n}{2}(\gamma-1)\sqrt{\Pi_1/\gamma}\frac{(kr)\left(\frac{l}{r}\right)\left(\frac{k_r}{k}\right)\left(\frac{k_r}{k_z}\right)}{i\tilde{\omega} + a(kr)^2[E]/\mathrm{Pr}}\right] = 0. \tag{41}$$

Here the dimensionless factors $[R]$, $[\Phi]$, $[Z]$ and $[E]$ have the form

$$[R] = \left[1 - i\alpha_{visc}\left(\frac{k_z^2-k_r^2}{kk_z}\right)\frac{1}{(kr)}\left(\frac{u_\phi}{u_s}\right)\right],$$
$$[\Phi] = \left[1 - i\alpha_{visc}\left(\frac{k_z}{k}\right)\frac{1}{(kr)}\left(\frac{u_\phi}{u_s}\right)\right],$$
$$[Z] = \left[1 - i2\alpha_{visc}\left(\frac{k_z}{k}\right)\frac{1}{(kr)}\left(\frac{u_\phi}{u_s}\right)\right],$$
$$[E] = \left[1 - i(c-d)\left(\frac{k_z}{k}\right)\frac{1}{(kr)}\left(\frac{u_\phi}{u_s}\right)\right]. \tag{42}$$

The inspection of Eq. (41) reveals the following properties of the solution:

- the solution should be independent on the radial direction of the perturbation wave since the radial component of the wave vector appears as k_r^2. Change of the sign of k_z reverses the sign of the real part of the solutions (see the second and third column in Fig. 1);
- in the limit of small viscosity, the second bracket in Eq. (41) becomes real in the first order, suggesting the stability. The decrease in the viscous instability increment with decreasing l/r is clearly seen in Fig. 3;
- for $u_s/u_\phi \sim 0.01$ (thin discs) and small $k_z/k \ll 1$, $k_r \sim 1$ and $kr \sim 10$, where the viscous instability appears (see below), the most appreciable correction is for the $[R]$-factor. However, in the dispersion equation (41) the term $(i\tilde{\omega} + a(kr)^2[R])$ is multiplied by the small value $(k_z/k)^2$, and therefore the effects from the correction factors $[R] - [E]$ on the solution of the dispersion equation should be not significant, as indeed we found to be the case.

This dimensionless dispersion equation for $\tilde{\omega}$ as a function of the dimensionless wavenumber (kr) is to be solved for different values of the dimensionless parameters: the Prandtl number Pr, which characterizes the effect of thermal conductivity, l/r and u_s/u_ϕ, which describe the viscosity, and k_r/k, which determines the direction of the wave (evidently, $(k_z/k)^2 = 1 - (k_r/k)^2$).

3.2 Numerical solution of the dispersion equation

In principle, it is possible to carry out analytical investigation of the properties of the solutions of the cubic equation Eq. (41), e.g. in a way similar to study of MRI modes by Pessah & Chan (2008). However, the main aim of the present paper is to show the existence of the viscous instability in shearing flows, therefore we will numerically solve Eq. (41) for different representative parameters. Everywhere below in this Section we shall consider the phenomenologically important Keplerian case with $n = 3$ and $\tilde{\varkappa} = 1$. This does not restrict our analysis, since the instability persists at any n but $n = 0$ (see the next Section).

3.2.1 Case of electron heat conductivity

We start with the electron heat conductivity in a fully ionized plasma. We remind that in this case the Prandtl number is Pr_e=0.052, the dynamical viscosity coefficient is $\eta \sim T^{5/2}$, the heat conductivity coefficient is $\kappa \sim T^{5/2}$, so that $\alpha_{visc} = 5/2$, $c = 5/2$ and $d = 0$ in Eq. (42). Fig. 1 shows the real (upper panels) and imaginary (bottom panels) parts of three solutions of the cubic dispersion equation Eq. (41) $\tilde{\omega}$ as a function of the dimensionless wavenumber kr. All three solutions of this equation are complex since the dispersion equation has complex coefficients. The dimensionless parameters are $u_s/u_\phi = 0.01$ (thin discs), $l/r = 0.01$ (the maximum possible free-path length of ions, not to exceed the disc thickness), $k_r/k = 0.999$ (the direction of perturbations with increment close to maximal one for these parameters, see Fig. 2). Two Rayleigh modes modified by viscosity are marked as R+ and R-, according to the sign of their real parts at $kr \to 0$. The first two columns show the solutions for $k_r = 0.999$ and positive $k_z > 0$ and negative $k_z < 0$, respectively. It is seen that the sign of k_z determines which of the Rayleigh modes, R+ or R-, becomes unstable. It is also seen the unstable mode is that which has the real part intersecting with the new X-mode (the latter is always stable, i.e. has a non-negative imaginary part, representing an oscillating wave). The unstable Rayleigh mode has a non-zero increment already for long perturbations with $kr \to 0$. It has a maximum increment of ~ 0.1 at $kr \approx 5$ and is stabilized by viscosity for $kr \gtrsim 25$.

Fig. 2 illustrates the effect of changing the perturbation propagation wavevector value k_r/k in the range from 0.9 to 0.9999. It is seen that at $k_r/k = 0.999$ the instability increment is about maximum (we did not investigate the exact value of k_r/k for maximum increment, which, if necessary, can be straightforwardly done by differentiating the dispersion equation with respect to k_r/k and equating the result to zero).

Fig. 3 shows the unstable Rayleigh R+ mode behaviour with changing the viscosity parameter l/r and other parameters fixed as in Fig. 2. It is seen that diminishing the particle free-path length from the maximum possible value ($l/r = 0.01$ in this case) by an order of magnitude decreases the Rayleigh R+ mode instability increment by about two times, but increases the instability interval from $kr \simeq 25$ to $kr \simeq 70$.

Fig. 3 also illustrates the effect of increasing or decreasing the disc thickness by three times ($u_s/u_\phi = 0.03$ and $u_s/u_\phi = 0.003$, respectively). The imaginary part of the unstable R+ mode is shown for three values of the viscosity parameter $l/r = 0.03$, 0.01 and 0.003. Note the close similarity (almost identity) of the curves to those in Fig. 3, but the stretching of the kr variable by three times. This reflects an almost self-similarity of the dispersion equation Eq. (41) with respect to the dimensionless viscosity $a(kr)^2 = (u_s/u_\phi)(l/r)(kr)^2$.

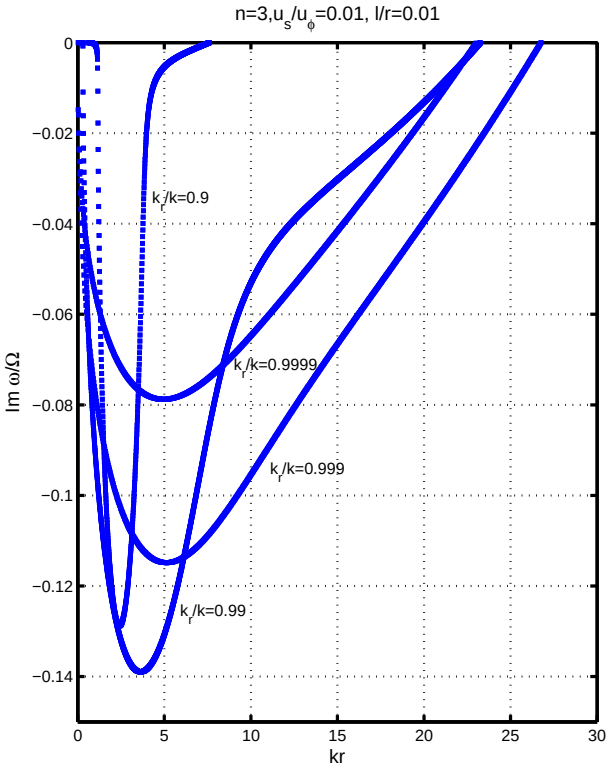

Figure 2. Imaginary part of the viscously unstable mode R+ in fully ionized gas with electron heat conductivity (Pr_e=0.052) and viscosity parameters $u_s/u_\phi = 0.01, l/r = 0.01$ for four values of the wave vector $k_r/k = 0.9$, 0.99, 0.999, and 0.9999.

3.2.2 Case of radiative heat conductivity

For a mixture of electrons and photons, the heat conductivity can be characterized of an effective Prandtl number defined as

$$\frac{1}{\mathrm{Pr}} \equiv \frac{1}{\mathrm{Pr}_\gamma} + \frac{1}{\mathrm{Pr}} = \frac{1}{\mathrm{Pr}}\left(1 + \frac{\mathrm{Pr}}{\mathrm{Pr}_\gamma}\right) = \frac{1}{\mathrm{Pr}_e}\left(1 + \frac{q_\gamma}{q_e}\right), \qquad (43)$$

where the heat flux due to electrons is

$$q_e = -\frac{1}{3} u_s l_e n_e \nabla(k_\mathrm{B} T) \qquad (44)$$

and the heat flux due to photons is

$$q_\gamma = -\frac{1}{3} c l_\gamma \nabla(a_\mathrm{r} T^4) \qquad (45)$$

where a_r is the radiation constant. Therefore,

$$\frac{q_\gamma}{q_e} \simeq \beta \frac{c}{u_s} \frac{z_0}{\tau} \sigma_{ei} n_e \qquad (46)$$

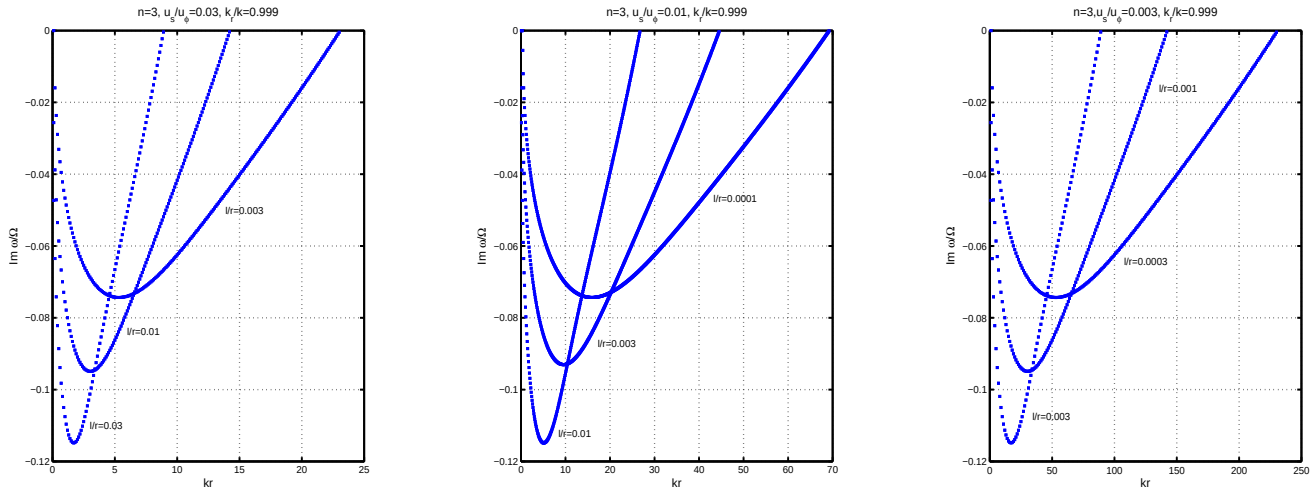

Figure 3. Almost precise self-similarity of the solution for different disc thickness parameters u_s/u_ϕ. Shown are three cases for Pr_e=0.052, $k_r/k = 0.999$ and (from left to right) $u_s/u_p hi = 0.03, 0.01, 0.003$ with different values of l/r. It is seen that the combination $a(kr)^2$ is almost exactly the same for all three figures.

where $\beta \equiv p_\gamma/p_{\rm gas}$ is the radiation to gas pressure ratio, τ is the effective optical thickness of the disc and σ_{ei} is the electron-ion interaction cross-section. Noticing that $n_e\sigma_{ei}u_s = \nu_{ei} = \Omega_{ei}/2\pi$ is the electron-ion collisional frequency, Eq. (46) can be recast into the form

$$\frac{q_\gamma}{q_e} \simeq \frac{\beta}{2\pi}\frac{\Omega_{ei}/\Omega}{\tau}\frac{c}{u_s}\,. \qquad (47)$$

Fig. 4 shows the effect of decreasing the effective Prandtl number due to increase of the radiation heat conductivity. Two cases with Pr=Pr_e/2, Pr_e/11 are shown in comparison with the case of electron heat conductivity only. It is seen that the radiation conductivity in fully ionized plasma strongly decreases (but does not vanish) the instability increment.

3.2.3 *Case of cold neutral gas*

Let us discuss the case of cold neutral gas. In this case the Prandtl number Pr_n=2/3 according to simplified kinetic theory (Hirschfelder, Curtiss & Bird 1954) and the heat conductivity coefficient $\kappa \sim T^{1/2}$ ($c = 1/2$, $d = 0$) (Spitzer 1962).

Fig. 5 shows the imaginary part of the unstable mode R+ for the standard parameters $u_s/u_\phi = 0.01$, $k_r/k = 0.999$ used above in the case of ideal neutral hydrogen gas with $\mathrm{Pr}_n = 2/3$ and the viscosity parameters $l/r = 0.01$ and $l/r = 0.03$. As above, the decrease in the particle free-path length widens the instability wavelength interval and decreases the instability increment. In this case, the instability increment is maximum at $kr \simeq 17$ and is about 0.18, almost two times as large as in the case of the purely electron heat conductivity in fully ionized gas discussed above. Therefore, the viscous instability turns out to be the most strong in the case of cold neutral gases.

4 SHEARED FLOWS WITH NON-KEPLERIAN ROTATION

Here we discuss the behaviour of the viscously unstable Rayleigh mode in flows with possible non-Keplerian rotation (i.e where $\Omega^2 \propto r^{-n}$ and $n \neq 3$). The solid-body rotation case with $n = 0$ was already discussed above. In that case there is no shear and the coefficients $A = B = 0$ in Eq. (31) but the viscosity remains in equations of motion (see the discussion at the beginning of Section 3).

The case of a Rayleigh-unstable flow with $n > 4$ (i.e. with specific angular momentum decreasing outward) is shown in Fig. 6. Here the R- mode is unstable (unlike in the Keplerian case with $k_z > 0$) in a wide range of kr with non-zero negative imaginary part at $kr \to 0$ and the maximum instability increment ~ 0.2.

Now consider a flow with increasing angular velocity with radius, i.e. with $n < 0$. As is well known, such flows are MRI-stable (Velikhov 1959; Chandrasekhar 1960). However, the viscous instability discussed in this paper persists in this case (see Fig. 7). Like in the case with $n = 6$, the R- mode is unstable in a wide range of kr.

Finally, the flow with constant angular momentum ($n = 4$) corresponds to $\varkappa = 0$ and deserves special consideration. Such flows can be realized in various astrophysical situations, e.g. in quasi-spherical accretion with angular momentum onto compact stars (Shakura et al. 2012). If the correction factors $[R] - [E]$ (42) were ignored, pure decay of perturbations due to viscosity would take place, $\omega = i\nu k^2$. However, if they are taken into account, the solution of Eq. (41) is

$$\omega = i\nu k^2 + \alpha_{visc}\nu k^2 \frac{k_z}{k}\frac{1}{(kr)^2}\frac{u_\phi}{u_s}\,, \qquad (48)$$

representing decaying oscillations with frequency $\sim \alpha_{visc}\Omega_K(lk_z)$, which can be much smaller than the Keplerian one.

5 DISCUSSION

5.1 Justification of the approximation of incompressibility

As is well known (see Landau & Lifshitz (1959)), the approximation of incompressibility requires the characteristic time of the density change in a fluid to satisfy the relation $\tau \gg L/c_s$, where L is the characteristic scale of the problem. For perturbations with the characteristic frequency $\omega = 2\pi/\tau$ and wavenumber $k = 2\pi/L$ this

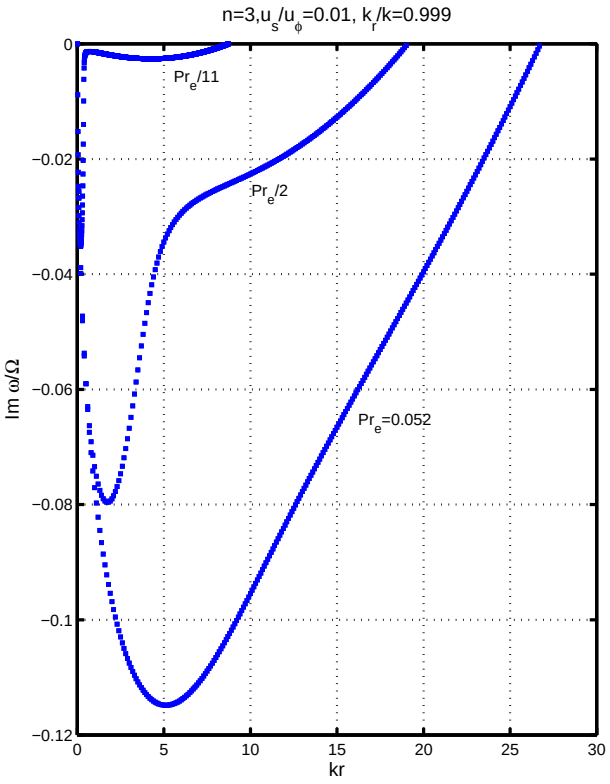

Figure 4. Imaginary part of the unstable mode R+ for $u_s/u_\phi = 0.01$, $l/r = 0.01$, $k_r/k = 0.999$ and different values of the effective Prandtl number (43), illustrating the effect of radiative conductivity growth.

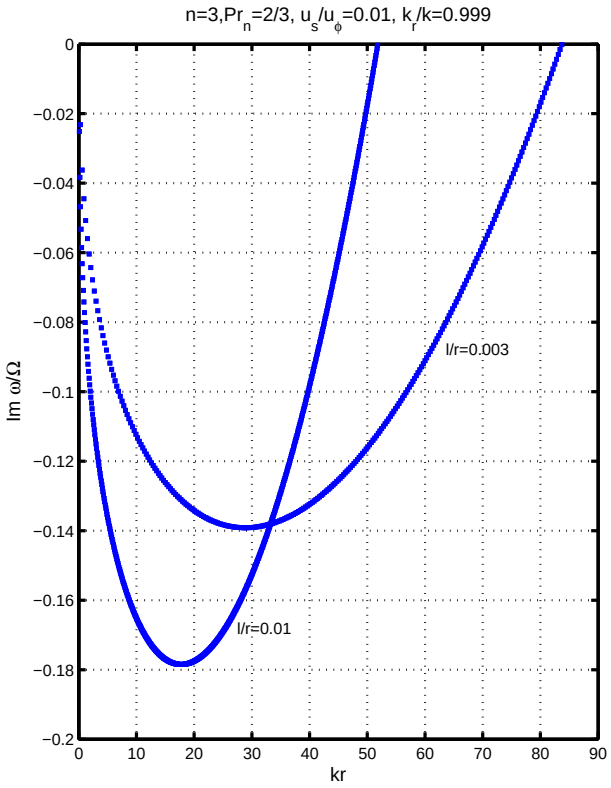

Figure 5. Imaginary part of the unstable mode R+ in the case of ideal neutral hydrogen gas with $\mathrm{Pr}_n = 2/3$ for $k_r/k = 0.999$, $u_s/u_\phi = 0.01$, and viscosity parameter $l/r = 0.01$.

general relation yields $\omega \ll kc_s$, and in the thin discs with $c_s \sim \Omega z_0$ we obtain the condition of the incompressibility in the form

$$kz_0 \gg \frac{\omega}{\Omega}\,. \tag{49}$$

Writing $kz_0 = (kr)(z_0/r) = (kr)(u_s/u_\phi)$, this condition becomes

$$(kr) \gg \frac{(\omega/\Omega)}{(u_s/u_\phi)}\,. \tag{50}$$

For thin discs with $u_s/u_\phi \sim 0.01 - 0.03$ and for the found mode frequencies $\omega \lesssim 0.1\Omega$ we see that the assumption of the incompressibility is valid for modes with $(kr) \gg 3 - 10$. This implies that in the range $(kr) \sim 10 - 50$ where the viscous instability considered here reaches maximum increments (especially in the case of cold neutral gases) the assumption of incompressibility is justified and sound wave modes can be ignored.

5.2 Damping by entropy gradients

So far we have ignored the possible radial and vertical entropy gradients, i.e. have dealt with locally adiabatic flow. As is well known (see, e.g., Kato, Fukue & Mineshige (1998)), the presence of non-zero entropy gradients $s_r \equiv \partial s/\partial r$ and $s_z \equiv \partial s/\partial z$ can stabilize instabilities. For example, if the vertical temperature gradient in a flow is non-adiabatic, $dT/dz < dT/dz_{ad} = g_z/C_p$, the restoring gravity force would suppress the development of convection, leading to an oscillatory vertical motion of a gas parcel with the Brunt-Väisälä frequency N_z. Qualitatively, it is expected that if this frequency is larger than the instability increment, the perturbation amplitude will not increase. To quantify this, we introduce the entropy gradients into the right-hand side of energy equation (7), and arrive at the modified dispersion equation:

$$\begin{aligned}(i\omega + \nu k^2[\Phi])\left[(i\omega + \nu k^2[R])\frac{k_z^2}{k^2} + (i\omega + \nu k^2[Z])\frac{k_r^2}{k^2}\right] \\ + \left(\frac{k_z}{k}\right)^2 \varkappa^2 \left[1 + \frac{(i\omega + \nu k^2[\Phi])}{(i\omega + \nu k^2[E]/\mathrm{Pr})}\frac{\left(N_r - \dfrac{k_r}{k_z}N_z\right)^2}{\varkappa^2}\right. \\ \left. - \frac{\gamma - 1}{\gamma}\frac{ik_r}{(i\omega + \nu k^2[E]/\mathrm{Pr})}\left(A - \frac{k_r}{k_z}B\right)\right] = 0\,.\end{aligned} \tag{51}$$

Here $N_r^2 = -S_r g_r$ and $N_z^2 = -S_z g_z$ are the Brunt-Väisälä frequencies. It is seen that it is the vertical Brunt-Väisälä frequency N_z that mostly affects the results, the radial oscillations being suppressed by small factor k_z/k_r. We find that in the case of Keplerian rotation of ionized ideal gas with Pr_e=0.052 and $k_r/k = 0.999$ the viscous instability discussed above disappears for $N_z/\Omega \gtrsim 0.3$. Neutral gas with Pr_n=2/3 is stabilized if $N_z \gtrsim 0.35$. For example, for a polytropic thin accretion discs with vertical structure described by the polytropic index n', $P = K\rho^{1+1/n'}$, discussed in Ketsaris & Shakura (1998), $N_z^2 = 2z^2(n' - 3/2)\Omega_K^2/(1 - z^2)$, where Ω_K is the Keplerian rotation frequency. The Brunt-Väisälä frequency N_z averaged over

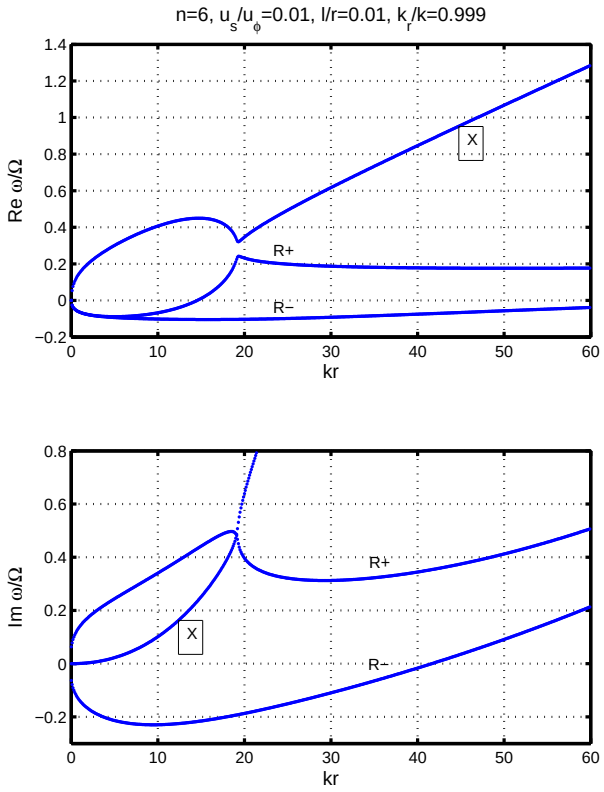

Figure 6. Three modes of dispersion equation Eq. (41) in the case of a Rayleigh-unstable flow with $n = 6$.

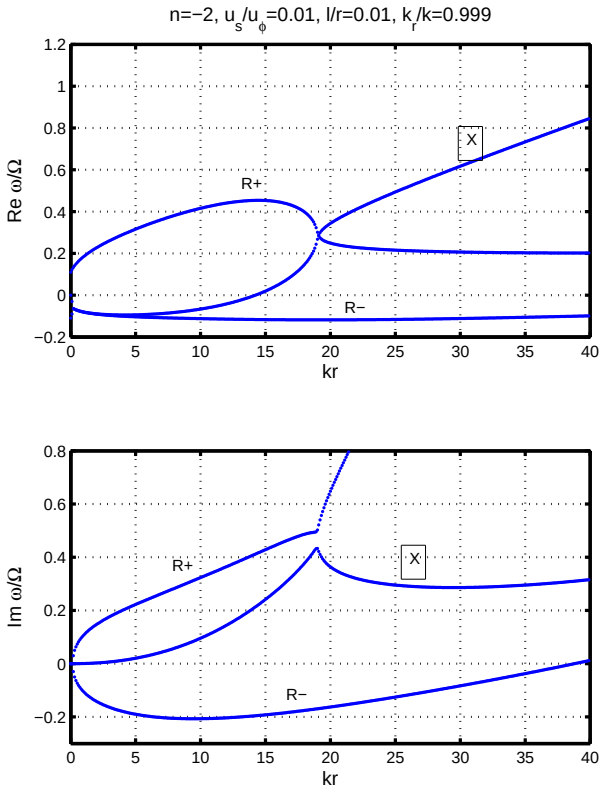

Figure 7. Three modes of dispersion equation Eq. (41) in the case of a flow with angular velocity linearly increasing with radius $\Omega \sim r$ ($n = -2$), which is stable against MRI.

the disc height z_0 is $\langle N_z/\Omega_K \rangle = \sqrt{(n' - 3/2)/2}$. Therefore, the value $N_z = 0.3$ corresponds to a polytropic index $n' \simeq 1.7$. Of course, realistic flows can be not polytropic, and therefore effects of the entropy gradients on the viscous instability should be investigated separately in each particular case.

6 SUMMARY AND CONCLUSION

In the present paper we have performed a linear local WKB analysis of time evolution of small axisymmetric perturbations in sheared hydrodynamic laminar flows. As a simplification, we have used the Boussinesq approximation for the description of the perturbations, but included the viscous dissipation and heat conductivity terms in the energy equation. This procedure led us to a third-order algebraic dispersion equation with complex coefficients (see Eq. (41)). The inclusion of these terms makes one of the Rayleigh modes (with positive or negative real part depending on the sign of the wavevector component k_z) unstable for long-wave perturbations for locally adiabatic case (i.e. ignoring local entropy gradients). The new X-mode of this cubic equation is found to be always stable (i.e. has a positive imaginary part).

We have studied numerically the behaviour of the unstable Rayleigh mode in the most interesting case of thin Keplerian accretion discs for different values of the viscosity (which is parametrized by the mean free-path length of ions), disc thickness (which is described by the ratio of the sound velocity to the unperturbed tangential velocity in the flow), the directions of the perturbation propagation (which is described by the ratio of wave vector components k_r/k_z), and the Prandtl numbers (which describe the heat conductivity effects). We have found that the value of heat conductivity mostly affect the instability increment, which is found to be maximum ~ 0.2 of the local Keplerian frequency in the case of cold neutral gas with the highest value of the Prandtl number $\mathrm{Pr}_n = 2/3$ (see Fig. 5). In the fully ionized gas characterized by the Prandtl number $\mathrm{Pr}_e = 0.052$ for purely electron heat conductivity, the instability increment is about 0.1 and decreases with increasing the role of the radiation heat conductivity (Fig. 4). The instability increment does not sensitive to the direction of propagation of perturbations (the sign of wavenumbers k_r and k_z) (Fig. 1) and persists as long as shear and viscosity are present in the flow and the flow is not iso-momentum when the epicyclic frequency vanishes, i.e. for any law of the angular momentum $\Omega^2 \sim r^{-n}$ (see Fig. 6 and Fig. 7).

In the presence of viscous dissipation, the instability arises when the pressure gradients along radial or vertical coordinates are non-zero, suggesting its convective nature: the heat generation in a sheared viscous flow in the gravity field of the central star makes the flow convectively unstable. Different aspects of convection in cold accretion discs, especially suitable for the physics of protoplanetary discs, has been addressed in many papers, starting from the pioneer paper by Lin & Papaloizou (1980) (see also Ryu & Goodman (1992); Lesur & Ogilvie (2010), and references therein).

We show that the incompressibility approximation is applica-

ble to describe small perturbations in thin accretion discs with not very long wavelength ($kr \gg 3-10$). At longer wavelengths, acoustic perturbations should be taken into account. On the other hand, the local WKB analysis is applicable only for $kr \gg 1$. Thus, the found instability with maximum increment at $kr \sim 10-50$ seems to be robust under our assumptions.

Thus we conclude that the viscous instability of one of the classical Rayleigh mode discovered in the present paper may be a seed for the development of turbulence in sheared flows which are hydrodynamically stable according to the classical Rayleigh criterion (i.e. in which the angular momentum increases with radius), or stable against MRI (e.g. flows with angular velocity increasing with radius). This instability is certainly worth investigating further.

7 ACKNOWLEDGEMENTS

We thank the anonymous referee for very useful stimulating notes. We acknowledge V.V. Zhuravlev and G.V. Lipunova for fruitful discussions and Max-Planck Institute for Astrophysics (MPA, Garching) for hospitality. The work is supported by the Russian Science Foundation grant 14-12-00146.

REFERENCES

Acheson D. J., 1978, Royal Society of London Philosophical Transactions Series A, 289, 459
Balbus S. A., Hawley J. F., 1991, ApJ, 376, 214
Balbus S. A., Hawley J. F., 1998, Reviews of Modern Physics, 70, 1
Blumenthal G. R., Lin D. N. C., Yang L. T., 1984, ApJ, 287, 774
Chandrasekhar S., 1960, Proceedings of the National Academy of Science, 46, 253
Eddington A. S., 1926, The Internal Constitution of the Stars. Cambridge: Cambridge University Press
Goodman J., Xu G., 1994, ApJ, 432, 213
Hirschfelder J. O., Curtiss C. F., Bird R. B., 1954, Molecular Theory of Gases and Liquids. J. Wiley and Sons, New York
Kato S., 1978, MNRAS, 185, 629
Kato S., Fukue J., Mineshige S., eds., 1998, Black-hole accretion disks. Kyoto: Kyoto University Press
Ketsaris N. A., Shakura N. I., 1998, Astronomical and Astrophysical Transactions, 15, 193
Kley W., Papaloizou J. C. B., Lin D. N. C., 1993, ApJ, 409, 739
Kotko I., Lasota J.-P., 2012, A&A, 545, A115
Kundu P. K., Cohen I. M., Dowling D. R., 2012, Fluid Mechanics, 5th edn. Academic Press, Boston
Landau L. D., Lifshitz E. M., 1959, Fluid mechanics. Oxford: Pergamon Press
Latter H. N., Ogilvie G. I., 2006, MNRAS, 372, 1829
Lesur G., Ogilvie G. I., 2010, MNRAS, 404, L64
Lin D. N. C., Papaloizou J., 1980, MNRAS, 191, 37
Pessah M. E., Chan C.-k., 2008, ApJ, 684, 498
Ryu D., Goodman J., 1992, ApJ, 388, 438
Shakura N., Postnov K., Kochetkova A., Hjalmarsdotter L., 2012, MNRAS, 420, 216
Shakura N. I., Postnov K. A., 2014, MNRAS in press. ArXiv e-prints 1412.1223
Shakura N. I., Sunyaev R. A., 1973, A&A, 24, 337
Spiegel E. A., Veronis G., 1960, ApJ, 131, 442
Spitzer L., 1962, Physics of Fully Ionized Gases. Interscience, New York
Suleimanov V. F., Lipunova G. V., Shakura N. I., 2008, A&A, 491, 267
Velikhov E. P., 1959, Sov. Phys. JETP, 36, 1398
Zhuravlev V. V., Razdoburdin D. N., 2014, MNRAS, 442, 870

APPENDIX A: LINEARIZATION OF VISCOUS FORCE IN DYNAMICAL EQUATIONS

In cylindrical coordinates for axisymmetric flows the viscous force components read (see e.g. Kato, Fukue & Mineshige (1998))

$$\mathcal{N}_r = \frac{1}{\rho}\left(\frac{1}{r}\frac{\partial(rt_{rr})}{\partial r} - \frac{t_{\phi\phi}}{r} + \frac{\partial t_{rz}}{\partial z}\right), \tag{A1}$$

$$\mathcal{N}_\phi = \frac{1}{\rho}\left(\frac{1}{r^2}\frac{\partial(r^2 t_{r\phi})}{\partial r} + \frac{\partial t_{z\phi}}{\partial z}\right), \tag{A2}$$

$$\mathcal{N}_z = \frac{1}{\rho}\left(\frac{1}{r}\frac{\partial(rt_{rz})}{\partial r} + \frac{\partial t_{zz}}{\partial z}\right). \tag{A3}$$

The viscous stress tensor components are:

$$t_{rr} = 2\eta\frac{\partial u_r}{\partial r} + (\zeta - \frac{2}{3}\eta)\nabla\cdot\boldsymbol{u}\,, \tag{A4}$$

$$t_{r\phi} = \eta r\frac{\partial(u_\phi/r)}{\partial r}\,, \tag{A5}$$

$$t_{rz} = \eta\left[\frac{\partial u_z}{\partial r} + \frac{\partial u_r}{\partial z}\right], \tag{A6}$$

$$t_{\phi\phi} = 2\eta\frac{u_r}{r} + (\zeta - \frac{2}{3}\eta)\nabla\cdot\boldsymbol{u}\,, \tag{A7}$$

$$t_{\phi z} = \eta\frac{\partial u_\phi}{\partial z}\,, \tag{A8}$$

$$t_{zz} = 2\eta\frac{\partial u_z}{\partial z} + (\zeta - \frac{2}{3}\eta)\nabla\cdot\boldsymbol{u}\,. \tag{A9}$$

(Here $\eta = \rho\nu$ is the dynamical viscosity, ζ is the second viscosity.).

Below unperturbed and perturbed components will be marked with indexes 0 and 1, respectively, and therefore

$$u_r = u_{r,1}, \quad u_\phi = u_{\phi,0} + u_{\phi,1}, \quad u_z = u_{z,1}, \quad \rho = \rho_0 + \rho_1, \quad \eta = \eta_0 + \eta_1, \quad T = T_0 + T_1\,. \tag{A10}$$

For perturbed variables ρ_1, $u_{(r,\phi,z),1}$, T_1 taken in the form of plane waves $\sim \exp(i\omega t - k_r r - k_z z)$ the partial derivatives simply becomes $\partial/\partial r = -ik_r$, $\partial/\partial z = -ik_z$. The dynamic viscosity of interest here is a function of temperature only, $\eta \sim T^{\alpha_{visc}}$, therefore

$$\frac{\partial\eta}{\partial r} = -\alpha_{visc}\eta_0\frac{T_1}{T_0}ik_r + \alpha_{visc}\frac{\eta_0}{T_0}\frac{\partial T_0}{\partial r}\,, \tag{A11}$$

$$\frac{\partial\eta}{\partial z} = -\alpha_{visc}\eta_0\frac{T_1}{T_0}ik_z + \alpha_{visc}\frac{\eta_0}{T_0}\frac{\partial T_0}{\partial z}\,, \tag{A12}$$

(By varying η, we neglected logarithmic dependence on temperature and density in the Coulomb logarithm).

A1 Radial component

Inserting the stress tensor components into Eq. (A1) yields

$$\mathcal{N}_r = \frac{1}{\rho}\left[\eta\frac{\partial^2 u_r}{\partial r^2} + \eta\frac{\partial^2 u_r}{\partial z^2} + \frac{\eta}{r}\frac{\partial u_r}{\partial r} - \eta\frac{u_r}{r^2} + 2\frac{\partial\eta}{\partial r}\frac{\partial u_r}{\partial r} + \frac{\partial\eta}{\partial z}\frac{\partial u_z}{\partial r} + \frac{\partial\eta}{\partial z}\frac{\partial u_r}{\partial z}\right]. \tag{A13}$$

After linearizing we find:

$$\mathcal{N}_{r,1} = \frac{1}{\rho_0}\left[-\eta_0 k^2 u_{r,1} - 2ik_r u_{r,1}\alpha_{visc}\frac{\eta_0}{T_0}\frac{\partial T_0}{\partial r} - ik_r u_{z,1}\alpha_{visc}\frac{\eta_0}{T_0}\frac{\partial T_0}{\partial z} - ik_z u_{r,1}\alpha_{visc}\frac{\eta_0}{T_0}\frac{\partial T_0}{\partial z}\right]. \tag{A14}$$

The second term is $\sim k_r/r$ and is small compared to the first term $\sim k^2$ and last two terms $\sim k_z/z$ (we remind that in thin discs considered here $z_0/r \sim u_s/u_{\phi,0} \ll 1$). Noticing that $u_{z,1}k_z + u_{r,1}k_r = 0$ from the continuity equation, we obtain:

$$\mathcal{N}_{r,1} = -\nu k^2 u_{r,1}[R] \tag{A15}$$

where the factor that takes into account the dependence of viscosity on temperature is defined as

$$[R] = 1 + i\frac{k_z^2 - k_r^2}{k_z k^2}\alpha_{visc}\frac{1}{T_0}\frac{\partial T_0}{\partial z}\,. \tag{A16}$$

A2 Tangential component

Substituting stress tensor components into Eq. (A2) yields:

$$\mathcal{N}_\phi = \frac{1}{\rho}\left[\eta\frac{\partial^2 u_\phi}{\partial r^2} + \eta\frac{\partial^2 u_\phi}{\partial z^2} + \frac{\eta}{r}\frac{\partial u_\phi}{\partial r} - \eta\frac{u_\phi}{r^2} + \frac{\partial\eta}{\partial r}\frac{\partial u_\phi}{\partial r} - \frac{\partial\eta}{\partial r}\frac{u_\phi}{r} + \frac{\partial\eta}{\partial z}\frac{\partial u_\phi}{\partial z}\right]. \tag{A17}$$

The linearizing leads to:

$$\begin{aligned}\mathcal{N}_{\phi,1} = \frac{1}{\rho_0}&\left[\left(-\alpha_{visc}\eta_0\frac{T_1}{T_0}ik_r + \alpha_{visc}\frac{\eta_0}{r}\frac{T_1}{T_0}\right)\frac{\partial u_{\phi,0}}{\partial r} - \alpha_{visc}\frac{\eta_0}{r^2}\frac{T_1}{T_0}u_{\phi,0} - \eta_0 k^2 u_{\phi,1} - ik_z\eta_0\frac{1}{T_0}\frac{\partial T_0}{\partial z}u_{\phi,1}\right]\\ &-\frac{1}{\rho_0}\frac{\rho_1}{\rho_0}\left[\left(\alpha_{visc}\frac{\eta_0}{T_0}\frac{\partial T_0}{\partial r} + \frac{\eta_0}{r}\right)\frac{\partial u_{\phi,0}}{\partial r} + \left(\frac{\alpha_{visc}}{r}\frac{\eta_0}{T_0}\frac{\partial T_0}{\partial r} - \frac{\eta_0}{r^2}\right)u_{\phi,0}\right].\end{aligned} \tag{A18}$$

All terms in the second square brackets are $\sim 1/r^2$ and can be neglected compared to terms in the first square brackets. The latter can be rewritten as the sum of two terms:

$$\mathcal{N}_{\phi,1} = \frac{1}{\rho_0}\frac{T_1}{T_0}\left[\left(-\alpha_{visc}\eta_0 ik_r + \alpha_{visc}\frac{\eta_0}{r}\right)\frac{\partial u_{\phi,0}}{\partial r} - \alpha_{visc}\frac{\eta_0}{r^2}u_{\phi,0}\right] - \nu k^2\frac{u_{\phi,1}}{u_{\phi,0}}\left(1 + ik_z\frac{1}{T_0}\frac{\partial T_0}{\partial z}\right)u_{\phi,0}\,. \tag{A19}$$

Here three terms in the first brackets are $\sim k_r/r$, $\sim 1/r^2$, $\sim 1/r^2$, respectively, compared to terms $\sim k^2$ in the second brackets, and hence can be neglected. Therefore, we are left with

$$\mathcal{N}_{\phi,1} = -\nu k^2 u_{\phi,1}[\Phi] \tag{A20}$$

where

$$[\Phi] = 1 + i\frac{k_z}{k^2}\alpha_{visc}\frac{1}{T_0}\frac{\partial T_0}{\partial z}\,. \tag{A21}$$

A3 Vertical component

Substituting the stress tensor components into Eq. (A3) yields:

$$\mathcal{N}_z = \frac{1}{\rho}\left[\eta\frac{\partial^2 u_z}{\partial r^2} + \eta\frac{\partial^2 u_z}{\partial z^2} + \left(\frac{\eta}{r} + \frac{\partial\eta}{\partial r}\right)\left(\frac{\partial u_z}{\partial r} + \frac{\partial u_r}{\partial z}\right) + 2\frac{\partial\eta}{\partial z}\frac{\partial u_z}{\partial z}\right]. \tag{A22}$$

The linearization of terms in the middle brackets yields terms $\sim k_r/r, k_z/r$ which are small compared to the term $\sim k^2$ arisen from the second derivatives. Terms $\sim k_z/z$ arisen from the linearization of the last term, however, should be retained. Therefore, we finally find:

$$\mathcal{N}_{z,1} = -\nu k^2 u_{z,1}[Z] \tag{A23}$$

where

$$[Z] = 1 + 2i\frac{k_z}{k^2}\alpha_{visc}\frac{1}{T_0}\frac{\partial T_0}{\partial z}\,. \tag{A24}$$